AT-1 is the ER membrane acetyl-CoA transporter and is essential for cell viability

Mary Cabell Jonas[1,2], Mariana Pehar[1] and Luigi Puglielli[1,2,3,*]

[1]Department of Medicine and [2]Cellular and Molecular Biology Program, University of Wisconsin-Madison, Madison, WI 53705, USA
[3]Geriatric Research Education Clinical Center, VA Medical Center, Madison, WI 53705, USA
*Author for correspondence (lp1@medicine.wisc.edu)

Accepted 15 June 2010
Journal of Cell Science 123, 3378-3388

doi:10.1242/jcs.068841

Summary

The transient or permanent modification of nascent proteins in the early secretory pathway is an essential cellular function that ensures correct folding and maturation of membrane and secreted proteins. We have recently described a new form of post-translational regulation of the membrane protein β-site APP cleaving enzyme 1 (BACE1) involving transient lysine acetylation in the lumen of the endoplasmic reticulum (ER). The essential components of this process are two ER-based acetyl-CoA:lysine acetyltransferases, ATase1 and ATase2, and a membrane transporter that translocates acetyl-CoA into the lumen of the ER. Here, we report the functional identification of acetyl-CoA transporter 1 (AT-1) as the ER membrane acetyl-CoA transporter. We show that AT-1 regulates the acetylation status of ER-transiting proteins, including the membrane proteins BACE1, low-density lipoprotein receptor and amyloid precursor protein (APP). Finally, we show that AT-1 is essential for cell viability as its downregulation results in widespread cell death and induction of features characteristic of autophagy.

Key words: AT-1, Acetyl-CoA, Lysine acetylation, Membrane transport, Autophagy, Neurodegeneration

Introduction

Our group has recently identified a new form of post-translational regulation of the membrane protein β-site APP cleaving enzyme 1 (BACE1), the rate-limiting enzyme for the generation of the Alzheimer's disease (AD) amyloid β-peptide (Aβ) from its precursor, APP (Costantini et al., 2007). The process involves transient acetylation of the highly disordered N-terminal globular domain of nascent BACE1 in the lumen of the endoplasmic reticulum (ER) by two acetyl-CoA:lysine acetyltransferases, which we named ATase1 and ATase2 (Ko and Puglielli, 2009). The acetylated intermediates of BACE1 are able to reach the Golgi complex, where they are deacetylated by a Golgi-resident deacetylase (Costantini et al., 2007). By contrast, non-acetylated intermediates are retained and degraded in a post-ER compartment – most probably the ER Golgi intermediate compartment (ERGIC) – by a mechanism that requires the serine protease proprotein convertase subtilisin kexin type 9 (PCSK9, also known as NARC-1) (Jonas et al., 2008). As a result, changes in the expression levels and activity of ATase1 and/or ATase2 (Ko and Puglielli, 2009) as well as PCSK9 (Jonas et al., 2008) influence both BACE1 metabolism and Aβ generation, which are directly involved in the pathogenesis of AD.

In addition to the two acetyltransferases ATase1 and ATase2, the acetylation of nascent BACE1 requires active transport of the highly charged and membrane-impermeable acetyl-CoA from the cytosol into the lumen of the ER. Acetyl-CoA is the donor of the acetyl group in the reaction of lysine acetylation and represents an essential biochemical requirement for the above events (Costantini et al., 2007).

In 1997, Kanamori et al. reported the identification of a new protein (AT-1) that appeared to affect the acetylation of complex gangliosides in the secretory pathway (Kanamori et al., 1997). The authors were interested in the Golgi-resident acetyltransferase responsible for the *O*-acetylation of complex gangliosides but, surprisingly, the new protein displayed a possible ER localization in addition to features that were consistent with membrane transporters rather than acetyltransferases. These included the presence of multiple membrane-spanning domains and a leucine-zipper motif. Additionally, when the effects of AT-1 overexpression were assessed in semi-intact cells, only ~5% of radiolabeled acetyl-CoA was found to be incorporated in glycolipids, suggesting that AT-1 activity preferentially affects non-lipid constituents (Kanamori et al., 1997).

As a result, the authors proposed a possible role as ER membrane acetyl-CoA transporter and named the new protein acetyl-Coenzyme A transporter 1 (AT-1) (Hirabayashi et al., 2004; Kanamori et al., 1997). However, no functional proof was provided regarding the biochemical activity or properties of this protein. AT-1 has homologs in lower organisms, including *Saccharomyces cerevisiae*, *Caenorhabditis elegans* and *Drosophila melanogaster* (Hirabayashi et al., 2004), and is upregulated as result of ER-induced stress, suggesting a possible role during the unfolded protein response (UPR) (Shaffer et al., 2004). Recent work has also shown that *AT-1* is upregulated in motor neurons of patients affected by sporadic amyotrophic lateral sclerosis (ALS) (Jiang et al., 2007) and mutated in patients affected by autosomal dominant spastic paraplegia-42 (SPG42) (Lin et al., 2008), suggesting an implication in neurodegenerative disorders.

Here, we report that AT-1 (also called solute carrier family 33 member 1, SLC33A1) is an ER membrane acetyl-CoA transporter. AT-1 regulates the acetylation of BACE1, LDLR, APP and other ER-based protein substrates, and is upregulated in the brain of late-onset (sporadic) AD patients. Importantly, we show that AT-1 is essential for cell viability because its downregulation results in widespread cell death and induction of features characteristic of autophagy. These studies point to a fundamental role of the ER-

Journal of Cell Science

based acetylation machinery in both physiological and pathological conditions.

Results

AT-1 is the ER membrane acetyl-CoA transporter

To assess whether AT-1 is responsible for the acetyl-CoA transport activity that we have identified and described in the ER membrane (Costantini et al., 2007), and to characterize its biochemical properties together with its disease-relevant functions, we generated several individual colonies of Chinese hamster ovary (CHO) cells that overexpress human AT-1 (Fig. 1A,B). Transgenic AT-1 displayed ER localization and was completely absent from Golgi fractions (Fig. 1C), which is consistent with our previous localization of the ER membrane acetyl-CoA transport activity (Costantini et al., 2007). Next, we assayed the acetyl-CoA transport activity in individual fractions from a subcellular fractionation gradient of control (non-transfected) cells. The assay was performed under native conditions and in the absence of detergents, which preserves biochemical properties as well as in vivo topographical orientation of the membranes (Carey and Hirschberg, 1981; Costantini et al., 2007; Ko and Puglielli, 2009; Puglielli et al., 1999a; Puglielli et al., 1999b). Fig. 1D shows that the acetyl-CoA transport activity was only observed in fractions corresponding to the ER and that the distribution pattern of AT-1 overlapped with the endogenous acetyl-CoA membrane transport activity. Additionally, when we compared the acetyl-CoA membrane transport activity of similar ER fractions generated from control and AT-1 overexpressing cells, we found a significant increase in the rate of acetyl-CoA translocation following AT-1 overexpression (Fig. 1E).

The above results demonstrate that AT-1 is restricted to the ER membrane where it overlaps with the endogenous acetyl-CoA transport activity observed in native membranes. They also indicate that overexpression of AT-1 results in increased translocation of acetyl-CoA into the ER lumen. These results are consistent with our previous report showing that ER- but not Golgi-membranes possess acetyl-CoA transport activity (Costantini et al., 2007). However, they do not provide definitive evidence that AT-1 is solely responsible for acetyl-CoA translocation across the ER membrane.

To prove that AT-1 is the ER membrane acetyl-CoA transporter, we purified transgenic Myc-tagged AT-1 from stably transfected cells (see Fig. 1B) by using an anti-Myc antibody covalently attached to aldehyde-activated agarose beads (anti-Myc column). Affinity-purified AT-1 was then reconstituted into artificial liposomes prior to biochemical assessment of transport activity. Reconstituted proteoliposomes displayed very high acetyl-CoA transport activity, which was absent in liposomes alone or in non-reconstituted proteoliposomes (Fig. 1F). Finally, activity was also absent when reconstitution was performed with the elution product of the anti-Myc column from control (non-transfected) cells (Fig. 1F; reconstitution without AT-1). The above results clearly indicate that AT-1 alone is sufficient for transport activity into an artificial liposomal system and support the conclusion that AT-1 is the ER membrane acetyl-CoA transporter.

Previous work with nucleotide–sugar transporters of the Golgi membrane, which are required for Golgi-based glycosylation of glycoproteins and glycolipids, has shown that they act as antiporters (Berninsone and Hirschberg, 2000; Hirschberg et al., 1998). As a result, the import of the nucleotide–sugar complex is inhibited with high specificity by the nucleotide moiety. To test whether this

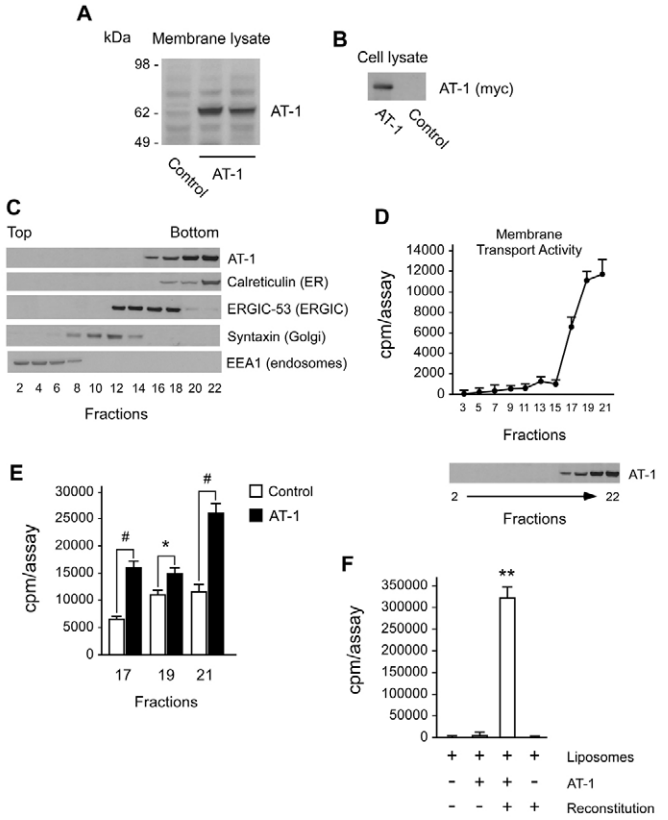

Fig. 1. AT-1 localizes in the ER and stimulates acetyl-CoA transport across the ER membrane. (**A**,**B**) Western blot analysis shows successful transfection of AT-1 into CHO cells. AT-1 migrates very close to the predicted molecular mass of 61 kDa. Transgenic AT-1 contained a Myc-His tag at the C-terminus and could be recognized with both anti-AT-1 (A) and anti-Myc (B) antibodies. (**C**) The subcellular distribution of transgenic AT-1 was analyzed by SDS-PAGE and immunoblotting after separation of intracellular membranes on a 10–24% discontinuous Nycodenz gradient. The appropriate subcellular markers are indicated. (**D**) Intracellular membranes from control CHO cells were prepared as described in C and then assayed for acetyl-CoA transport activity. Results are the average + s.d. (n=3). The distribution pattern of AT-1 as shown in C is shown here again to allow comparison with the biochemical activity of the single fractions. (**E**) The indicated ER fractions from control CHO cells (non-transfected) and cells stably transfected with AT-1 were assayed for acetyl-CoA transport. Results are the average + s.d. (n=3). (**F**) Affinity purified AT-1 was reconstituted into artificial liposomes prior to assessment of acetyl-CoA transport. Results are the average + s.d. (n=3). *P<0.05; $^{\#}P$<0.005; **P<0.0005.

was also the case for AT-1, we assessed the ability of CoA and other non-related molecules to inhibit translocation of acetyl-CoA into the lumen of purified ER vesicles. Fig. 2A,B shows that only CoA was able to reduce acetyl-CoA translocation across the ER membrane in a dose-dependent fashion. Importantly, no effect was observed when ER vesicles were incubated together with acetyl-CoA and ATP, UDP-galactose or Na-acetate (Fig. 2B). ATP is actively transported into the ER and Golgi lumen by two specific membrane transporters, whereas UDP-galactose is transported into the Golgi lumen by a Golgi-based membrane transporter (Berninsone and Hirschberg, 2000; Hirschberg et al., 1998). Therefore, the fact that neither was able to interfere with the translocation of acetyl-CoA indicates that the inhibition shown in

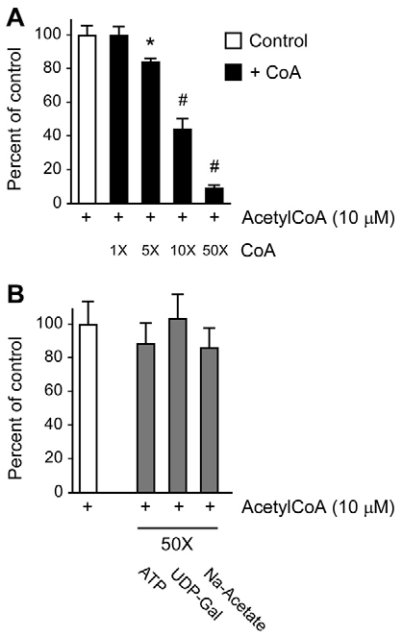

Fig. 2. Acetyl-CoA transport across the ER membrane is inhibited by CoA. (**A**) ER vesicles were assayed for acetyl-CoA transport in the presence or absence of increasing concentrations of CoA. Results are expressed as percent of control (no CoA; white bar) and are the average (n=3) + s.d. (**B**) The experiment described in A was repeated in the presence of ATP, UDP-galactose (UDP-Gal) or Na-acetate. *P<0.05; $^{\#}P$<0.005.

Fig. 2A is specific for CoA. Finally, the inability of Na-acetate, the sodium salt of acetic acid, to inhibit acetyl-CoA transport suggests that the CoA moiety of acetyl-CoA serves as the recognition signal for AT-1.

Downregulation of AT-1 causes ER expansion and autophagic cell death

To further analyze its function in vivo, we downregulated AT-1 by using small interfering RNA (siRNA) targeted against *AT-1*. Although reduced levels of *AT-1* mRNA were already evident 2 days after siRNA treatment (Fig. 3A), robust changes in the protein levels could only be observed after 6 days of treatment, suggesting a long half-life of the transporter (Fig. 3B). Surprisingly, the downregulation of AT-1 was accompanied by widespread cell death as assessed by conventional field microscopy (Fig. 3C), calcein incorporation into living cells (Fig. 3C), and direct counting of cells stained with a live-dead assay (Fig. 3D,E). Such an effect was not observed when cultures were treated with non-silencing siRNA (Fig. 3C–E) or with other non-related siRNAs previously used (Costantini et al., 2006; Jonas et al., 2008; Ko and Puglielli, 2007). These results should be viewed together with the fact that downregulation of AT-1 in zebrafish causes developmental defects and death (Lin et al., 2008). Additionally, apparent haploinsufficiency of *AT-1* is associated with autosomal dominant SPG42 (Lin et al., 2008), a human disease that is caused by degeneration of motor neurons in the corticospinal tract. When taken together, the above results clearly point to a fundamental role of AT-1 in the physiology of the cell.

To further advance our understanding of the mechanisms of cell death, we used transmission electron microscopy. Fig. 4A shows a collection of cellular features that are reminiscent of different

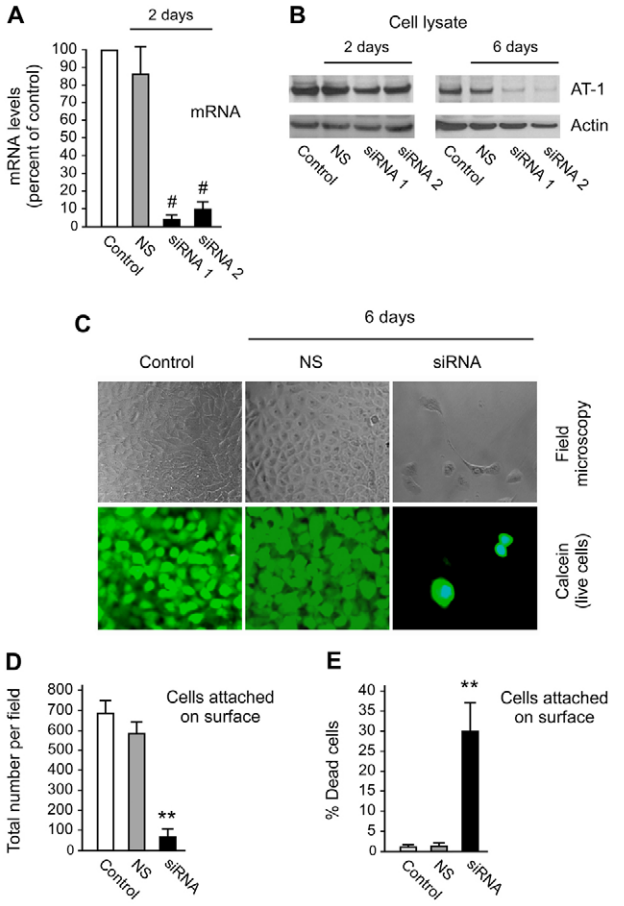

Fig. 3. Downregulation of AT-1 causes cell death. (**A**,**B**) H4 cells were treated with two siRNAs targeting *AT-1* prior to real-time quantification of *AT-1* mRNA levels (A) and western blot analysis of endogenous AT-1 (B). Results for A are the average + s.d. (n=6). (**C–E**) H4 cells were treated with siRNA targeting *AT-1* for 6 days and then analyzed for cell death. (C) Conventional field microscopy and calcein (green) incorporation for the visualization of living cells. (D) Direct quantification of calcein-stained cells attached on the dish after 6 days of siRNA treatment. (E) Attached cells were labeled with the Live/Dead viability Cytotoxicity Kit for Mammalian Cells for the visualization of live and dead cells. Results are expressed as percentage of dead cells over total number of cells attached to the dish. Results are the average + s.d. (n=9). NS, non-silencing siRNA; siRNA1 and siRNA2, two different siRNAs targeting *AT-1*. siRNA in D and E indicates the average of siRNA1 and siRNA2. $^{\#}P$<0.005; **P<0.0005.

stages of autophagic cell death (see panels a–d). In rare cases, the autophagic features coexisted with apoptosis-like chromatin condensation, suggesting activation of both autophagy- and apoptosis-dependent pathways (Fig. 4A; panels e and f). However, it must be noted that we were unable to detect caspase activation or poly(ADP-ribose) polymerase(PARP) cleavage (data not shown). This might reflect the fact that the vast majority of dying cells did not display apoptosis-like features when analyzed by electron microscopy. The activation of autophagic cell death was also associated with the upregulation of the autophagic markers beclin, LC3 and ATG5 (Fig. 4B). The presence of enlarged ER tubular structures was among the earliest events that we could detect following siRNA-mediated downregulation of AT-1 (Fig. 4C). This was often accompanied by a few autophagosomes (Fig. 4C), which

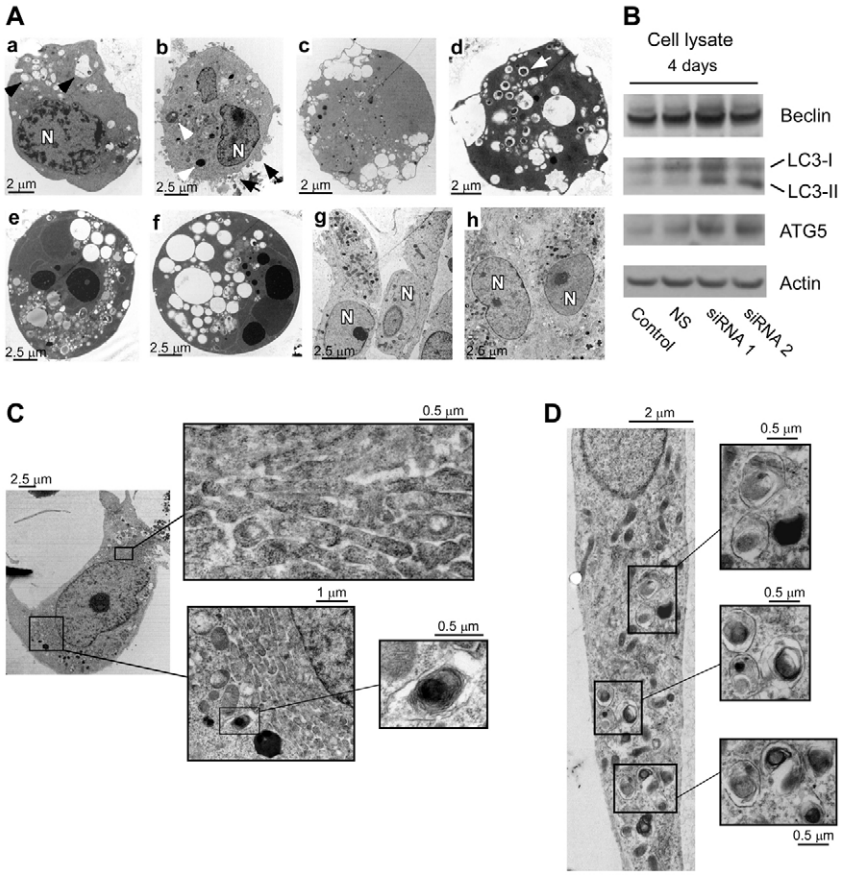

Fig. 4. The downregulation of AT-1 causes autophagic cell death. (**A**) H4 cells were treated with siRNA targeting *AT-1* prior to transmission electron microscopy. Panels a–d show a collection of cellular features that are reminiscent of different stages of autophagic cell death. Dying cells have a spherical appearance and differ dramatically from healthy cells (panels g and h). Panels a and b show cells with cellular blebbing (black arrows), visible nuclei (labeled N) and several vacuoles (black arrowheads) together with lysosomal proliferation (white arrowheads). The nucleus displays membrane invagination and modest chromatin clustering. The chromatin clustering appears as loose speckles and irregular peripheral bundles rather than the typical apoptosis-like condensation (compare with panels e and f). Panels c and d show cells with very large vacuoles, no visible organelles and ruptures of the plasma membrane. In many cases the vacuoles contain dense lysosomal material that corresponds to autophagosomes (see panel d, white arrow). These features correspond to the classic autophagic cell death. Cells in panels a and b reflect early stages, whereas cells in panels c and d reflect late stages of the process. In rare cases (panels e and f) the vacuoles and autophagosomes were accompanied by significant chromatin condensation. In these cases the chromatin condensation differed from that observed in panels a and b, and appeared similar to the more typical apoptosis-like condensation. These cells might reflect co-activation of both autophagic and apoptotic events. Non-treated control cells are shown in panel g, whereas panel h shows cells treated with non-silencing siRNA; in both cases cells display normal features. (**B**) Western blot analysis of total cell lysates shows upregulation of the autophagy markers beclin, LC3-I, LC3-II and ATG5 after siRNA-mediated downregulation of AT-1. NS, non-silencing siRNA; siRNA1 and siRNA2, two different siRNAs targeting AT-1. (**C**,**D**) Transmission electron microscopy of H4 cells following siRNA-mediated downregulation of AT-1. Images show early changes, prior to the widespread autophagic cell death described in A. ER enlargement (upper panel) together with autophagosomes in close proximity of the ER membrane (lower panel) are evident in C, and severe accumulation of autophagosomes throughout the cytosol is evident in D.

became very abundant in later stages (Fig. 4D). The autophagosomes were, at least initially, in close proximity to the ER, most probably because the ER membrane itself appears to be involved in the generation of the autophagic membrane (Axe et al., 2008). Finally, no morphological alterations of other organelles were observed at this stage, suggesting that the autophagy is triggered by ER-dependent events.

AT-1 regulates the acetylation status of several ER-based proteins

The results described above suggest that the cell needs a constant supply of acetyl-CoA into the lumen of the ER. This is most probably owing to the fact that acetyl-CoA serves as the donor of the acetyl group for the ε-amino acetylation of lysine residues on ER-transiting and, possibly, ER-resident proteins. Our previous results indicate that increased translocation of acetyl-CoA across the ER membrane favors the lysine acetylation of nascent BACE1 in the lumen of the ER, thereby resulting in increased cellular levels of BACE1 (Costantini et al., 2007). Consistently, $BACE1_{Gln}$ – a gain-of-acetylation mutant form of BACE1 where the lysine residues that are acetylated in the ER lumen (K126, K275, K279, K285, K299, K300, K307) are mutated to glutamine to mimic the effect of lysine acetylation (Masumoto et al., 2005) – displayed resistance to PCSK9 degradation (Jonas et al., 2008), rapid translocation along the secretory pathway and a longer half-life (Costantini et al., 2007). The opposite was true for the loss-of-acetylation mutants $BACE1_{Ala}$ and $BACE1_{Arg}$ (Costantini et al., 2007; Jonas et al., 2008).

To test whether AT-1 can regulate BACE1 metabolism, we analyzed the levels of endogenous BACE1 in CHO cells that

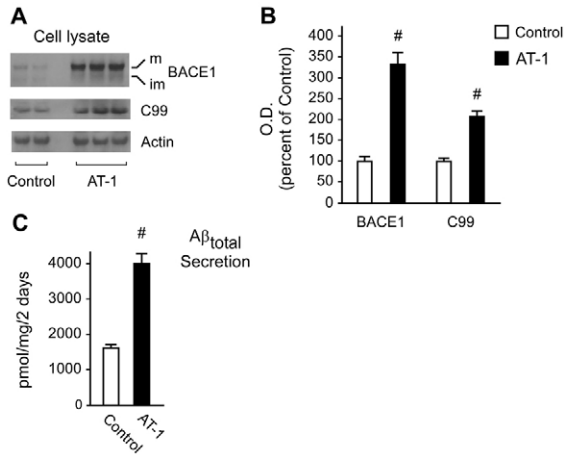

Fig. 5. Overexpression of AT-1 upregulates the steady-state level of BACE1 and the generation of Aβ. (**A**,**B**) Control CHO cells (non-transfected) and CHO cells stably transfected with AT-1 were analyzed for BACE1 levels and APP processing. A representative western blot is shown in A, whereas image quantification of changes [optical density (O.D.)] is shown in B. Results are the average + s.d. (n=6). (**C**) ELISA determination of total Aβ in the conditioned medium of control CHO cells and CHO cells stably transfected with AT-1. No effect was observed on the $A\beta_{total}$:$A\beta_{42}$ ratio (data not shown). Results are the average + s.d. (n=3). $^{\#}P<0.005$.

overexpress AT-1. Fig. 5A,B shows that BACE1 levels were greatly increased (~3.5-fold) in AT-1 overexpressing cells when compared with control (non-transfected) cells; this was also paralleled by increased levels of the APP C-terminal fragment C99 (Fig. 5A,B) and Aβ (Fig. 5C). C99 is the immediate product of BACE1-mediated cleavage of APP, whereas Aβ represents one of the final products of the sequential processing of APP by BACE1 and γ-secretase (Puglielli, 2008). Parallel changes in C99 and Aβ directly reflect the steady-state level and activity of BACE1. Taken together, the above results indicate that AT-1 levels and activity affect the metabolism of BACE1 and the rate of Aβ generation.

We initially discovered the ER-based acetylation machinery while studying the mechanisms that regulate BACE1 metabolism (Costantini et al., 2007). However, we recently reported that the nascent form of the low-density lipoprotein receptor (LDLR) is also acetylated in the ER (Jonas et al., 2008). To test the possibility that additional substrates are also affected by this new form of post-translational regulation, we analyzed the lysine acetylation profile of highly purified native ER vesicles. The experiment was performed in the presence or absence of trypsin to eliminate non-integral ER proteins associated with and/or bound to the cytosolic face of the organelle. This strategy, which was successfully used to confirm the topology of BACE1 acetylation (Costantini et al., 2007), allowed us to differentiate between the lysine acetylation occurring in the lumen of the ER from that potentially occurring on the cytosolic face of the organelle. In fact, as with the membrane transport assay (see Fig. 1D,E), vesicles were sealed and of the same in vivo topographical orientation (see also Costantini et al., 2007; Ko and Puglielli, 2009). As such, in the absence of detergent, trypsin does not have access to the lumen of the ER vesicles (see Fig. 6A). When performed under these conditions, the antibody directed to acetylated lysine residues recognized several ER-associated bands that were resistant to trypsin digestion (Fig. 6B), indicating that the acetylated lysine residues are located in the lumen of the ER. Importantly, we could not detect any acetylated protein band when trypsin digestion was performed in the presence of detergent (Fig. 6B), which allowed trypsin to access the ER lumen (see Fig. 6A for details). As expected, acetylated proteins were greatly reduced in highly purified intact Golgi vesicles. In fact, as with BACE1 and LDLR, membrane and/or secreted proteins are expected to be acetylated in the ER and deacetylated in the Golgi complex (Costantini et al., 2007; Jonas et al., 2008).

It is estimated that ~95% of proteins associated with the Golgi complex are transiting proteins, while the remaining 5% (or less) are Golgi resident proteins (Farquhar and Hauri, 1997). Golgi transiting proteins are almost exclusively membrane and secreted proteins that undergo post-translational modification in the lumen of the Golgi complex while trafficking from the ER to their final destination (Farquhar and Hauri, 1997). As a result, the electrophoretic profiles of ER and Golgi proteins are very similar with respect to number and separation of bands (Yunghans et al., 1970). Therefore, it is unlikely that the different acetylation profile of ER and Golgi vesicles shown in Fig. 6B is due to changes in protein composition of the organelles and not to the transient nature of the lysine modification itself (Costantini et al., 2007). However, to prove that the vesicles used in Fig. 6B did not have an abnormal composition, we assessed the electrophoretic profile of our ER and Golgi preparations by SDS-polyacrylamide gel electrophoresis (SDS-PAGE) and Coomassie staining. Although minor differences were evident, the pattern for ER and Golgi vesicles was very similar (Fig. 6C). This is in striking contrast to the acetylation pattern of the same vesicles (Fig. 6B; compare ER and Golgi in the absence of trypsin and Triton X-100), supporting our early conclusion that nascent transiting proteins are acetylated in the ER and deacetylated in the Golgi complex (Costantini et al., 2007; Jonas et al., 2008).

We next compared the lysine acetylation profile of ER vesicles purified from control, ceramide-treated and AT-1 overexpressing cells. Both ceramide treatment (Costantini et al., 2007) and AT-1 overexpression (Fig. 1) increase the import of acetyl-CoA into the ER lumen. As such, they are also predicted to increase the ER-based lysine acetylation. Fig. 6D,E clearly indicates that both ceramide treatment and overexpression of AT-1 increased the lysine acetylation of the ER vesicles (Fig. 6D,E). It is worth stressing that several proteins were consistently identified in the different experimental settings (indicated by lines in Fig. 6D,E).

Although it could be claimed that, in the absence of direct identification, the protein bands shown in Fig. 6 represent background, it is difficult to conceive that background protein bands are resistant to trypsin digestion in the absence of detergent (Fig. 6B), only evident in ER vesicles (Fig. 6B), and affected by both ceramide treatment (Fig. 6D) and AT-1 overexpression (Fig. 6E). Finally, we identified two of the acetylated bands indicated (arrowhead and asterisk in Fig 6D,E) as the immature and ER-based forms of BACE1 and LDLR, respectively (Fig. 6F). When taken together, the above results clearly indicate that AT-1 controls the post-translational lysine acetylation of several ER-based proteins.

APP is a substrate of the ER-based acetylation machinery

We have previously reported that the non-acetylated intermediates of both BACE1 and LDLR are disposed of by PCSK9 (Jonas et al., 2008). A recent report indicates that overexpression of APP in human neuroglioma (H4) cells reduces PCSK9-mediated disposal of LDLR (Abisambra et al., 2009). These preliminary results

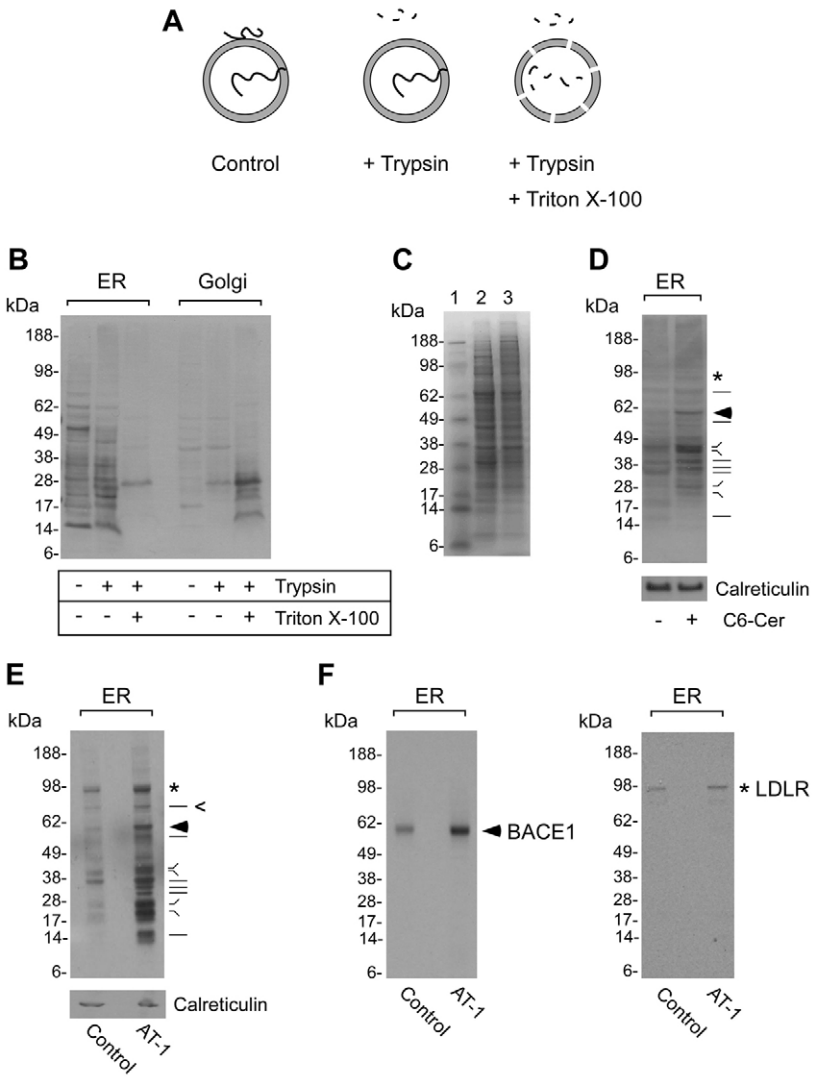

Fig. 6. Overexpression of AT-1 results in increased acetylation of ER proteins. (**A**,**B**) Intact ER and Golgi vesicles were digested with trypsin for 30 minutes at 25°C, in the presence or absence of 0.05% Triton X-100. Digestion was halted by adding an anti-trypsin-specific inhibitor. Triton X-100 was added to allow access of trypsin to the lumen of the vesicles. A schematic view of the rationale of this experiment is shown in A. Proteins were separated by SDS-PAGE and analysed by western blotting using an antibody against acetylated lysine. (**C**) The protein profile of the ER and Golgi vesicles used in B was assessed by SDS-PAGE and Coomassie staining. Lane 1, molecular markers; lane 2, ER; lane 3, Golgi complex. (**D**) Western blot assessment of the lysine-acetylation profile of intact ER vesicles purified from control (non-treated) and ceramide-treated (C6-cer; 10 μM) cells. Cells used here did not overexpress AT-1. The ER protein calreticulin was used as loading control. (**E**,**F**) Western blot assessment of the lysine-acetylation profile of intact ER vesicles purified from control (non-transfected) and AT-1 overexpressing cells. The membrane was initially blotted with an antibody against acetylated lysine (E) and then with antibodies against BACE1 (F, left panel) and LDLR (F, right panel). The ER protein calreticulin was used as loading control.

indicate functional competition between different substrates. In fact, transgenic APP (when overexpressed) can theoretically compete with endogenous LDLR, skewing PCSK9 towards APP (rather than LDLR) non-acetylated intermediates. However, for this to be the case, APP would need to be a substrate of the ER-based acetylation machinery. The presence of an acetylated band migrating with the apparent molecular mass of immature APP (Fig. 6E, indicated by the symbol <) would be consistent with such a possibility. To test this hypothesis, we immunoprecipitated APP from a total-cell lysate and analyzed whether APP can be detected with an antibody against acetylated lysine. Only the immature form of APP was found acetylated (Fig. 7A, right panel). Importantly, the upper two bands, which correspond to the mature species of APP (Fig. 7A, left panel), were not acetylated, mimicking the behavior previously described for both BACE1 and LDLR (Costantini et al., 2007; Jonas et al., 2008; Ko and Puglielli, 2009). Next, we assessed whether overexpression of AT-1 increased the levels of the ER-based nascent form of APP. Fig. 7B clearly shows increased levels of immature APP in ER vesicles purified from AT-1 overexpressing cells. To further prove that APP is a substrate of the ER-based acetylation machinery, a protein extract of highly purified ER vesicles was immunoprecipitated with an antibody against acetylated lysine and then analyzed by immunoblotting with an anti-APP antibody. Fig. 7C shows the presence of the immature form of APP in the immunoprecipitate, which supports an acetylated status. Similar results were obtained with LDLR (Fig. 7D) and BACE1 (Fig. 7E), for which the acetylation status has already been proven (Costantini et al., 2007; Jonas et al., 2008; Ko and Puglielli, 2009). Finally, we analyzed whether APP levels are affected by the genetic disruption of *Pcsk9*. In fact, the non-acetylated intermediates of both BACE1 and LDLR – currently the only two known substrates of the ER-based acetylation machinery – are disposed of by the serine protease PCSK9. As a result, their levels are increased in *Pcsk9*$^{-/-}$ mice (Jonas et al., 2008; Rashid et al., 2005). Increased levels of APP were found in the neocortex of *Pcsk9*$^{-/-}$ mice, thus supporting our hypothesis (Fig. 7F).

Therefore, the above results indicate that APP represents a substrate of the ER-based acetylation machinery. When taken together, the results support the conclusion that the ER-based acetylation of the ε-amino group of lysine residues is not limited to BACE1 or LDLR (Figs 6, 7). Future identification and characterization of all the different substrates will help define the impact of the ER-based lysine acetylation to the biology of the cell.

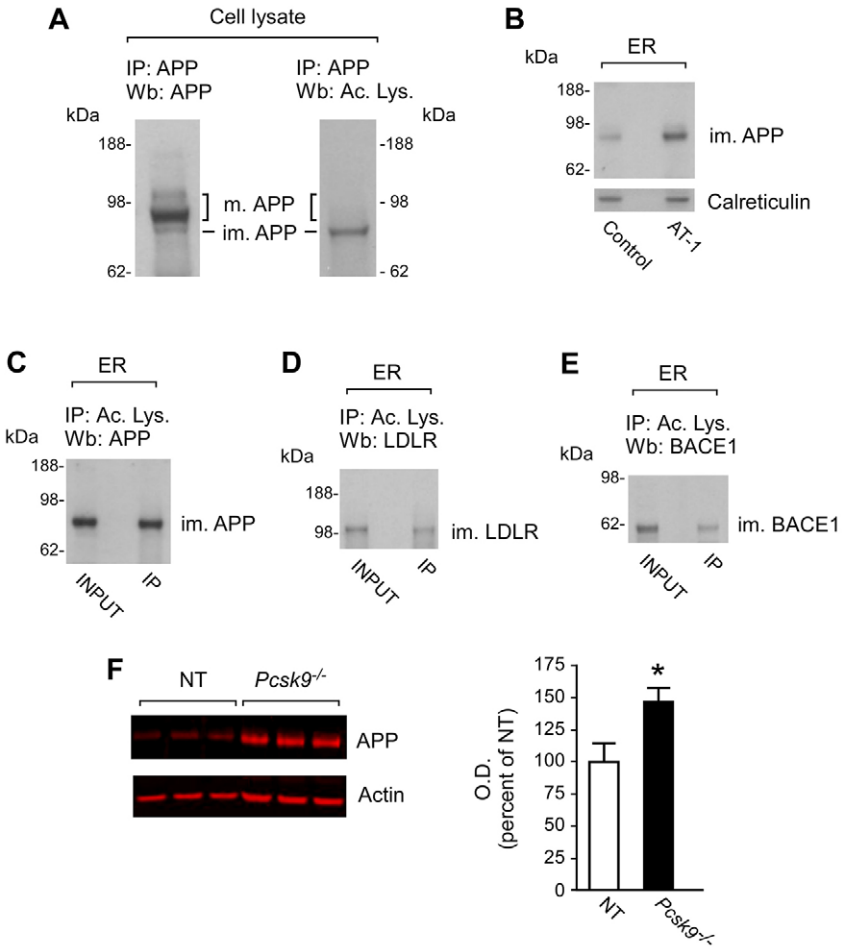

Fig. 7. APP is a substrate of the ER-based acetylation machinery. (**A**) Total cell lysates were immunoprecipitated with an anti-APP antibody and then analyzed with both anti-APP (left panel) and anti-acetylated lysine (right panel) antibodies. Only the ER-based nascent form of APP (im. APP, immature APP) was acetylated; m. APP, mature forms of APP. (**B**) Protein extracts from highly purified ER vesicles of control (non-transfected) and AT-1 overexpressing cells were analyzed for APP levels by western blot. The ER protein calreticulin was used as loading control. (**C**) Protein extracts from highly purified ER vesicles were immunoprecipitated with an antibody against acetylated lysine and then analyzed by western blotting using anti-APP antibody. (**D**,**E**) The experiment described in C was repeated with LDLR (D) and BACE1 (E) to show that APP behaves as LDLR and BACE1, currently the only two known membrane proteins undergoing transient acetylation in the lumen of the ER. im. LDLR, immature form of LDLR; im. BACE1, immature form of BACE1. (**F**) APP levels in the neocortex of non-transgenic (NT) and *Pcsk9*$^{-/-}$ animals were analyzed by immunoblotting with an anti-APP antibody. Imaging was performed with the LiCor Odyssey Infrared Imaging System. A representative western blot is shown in the left panel, and image quantification of changes [optical density (O.D.)] is shown in the right panel. Results are the average + s.d. (n=9). *P<0.05.

AT-1 is tightly regulated by the lipid second messenger ceramide

We have previously shown that the lipid second messenger ceramide can stimulate the acetylation of nascent BACE1 by increasing both the maximum velocity (V_{max}) of acetyl-CoA translocation across the ER membrane (Costantini et al., 2007) and the expression levels of the acetyltransferases ATase1 and ATase2 (Ko and Puglielli, 2009). To assess whether the increased import of acetyl-CoA in the lumen of the ER (Costantini et al., 2007) is a result of increased expression of AT-1, we treated CHO cells, H4 cells and mouse primary neurons with 10 μM ceramide, following a protocol that has already been described in detail (Costantini et al., 2007; Ko and Puglielli, 2009; Puglielli et al., 2003). Treatment resulted in a marked increase in the mRNA levels of *AT-1*, as detected by quantitative real-time PCR (Fig. 8A–C). Previous work has shown that ceramide levels in the mouse brain increase spontaneously during aging (Costantini et al., 2005) and are higher in *p44*$^{+/+}$ transgenic mice (Costantini et al., 2006), a progeroid animal model that resembles an accelerated form of aging (Maier et al., 2004) and develops premature cognitive deficits as well as an accelerated form of AD-like neuropathology (Pehar et al., 2010). Consistently, quantitative real-time determination of *At-1* mRNA levels in the brain of *p44*$^{+/+}$ transgenic animals revealed a ~2.5-fold increase when compared with both non-transgenic and heterozygous *p44*$^{+/-}$ mice (Fig. 8D). It is already known that the progeroid phenotype caused by the overexpression of p44 (also called DNp53) is only evident in the homozygous animals (Maier et al., 2004). As a result, heterozygous *p44*$^{+/-}$ mice have normal life-spans (Maier et al., 2004) and normal levels of ceramide and BACE1 (Costantini et al., 2006). We have previously shown that the levels of ceramide on the cell surface of mouse primary neurons increase spontaneously as the culture ages (Costantini et al., 2006). As such, we decided to assess the levels of *At-1* in both 'young' (day 3) and 'old' (day 24) neuronal cultures, following an experimental strategy that we have already described (Costantini et al., 2006). Both real-time mRNA quantitation and western blotting showed that old neurons had increased levels of *At-1* (Fig. 8E).

When taken together, the above results indicate that expression levels of AT-1 are tightly regulated by the second messenger ceramide; they also explain our previous finding that ceramide regulates acetyl-CoA import into the ER lumen (Costantini et al., 2007) and the increased acetylation pattern of ER-based proteins shown in Fig. 6D. The fact that the same results were obtained following spontaneous upregulation (Fig. 8D,E) and exogenous administration (Fig. 8A–C) of ceramide strengthen our conclusions. Finally, similar results were obtained with cell lines, primary neurons and brain tissue, clearly indicating that the above events are not limited to a specific cell type or to ex vivo experimental conditions.

Previous work has also shown that late-onset (sporadic) AD patients display increased levels of ceramide (approximately

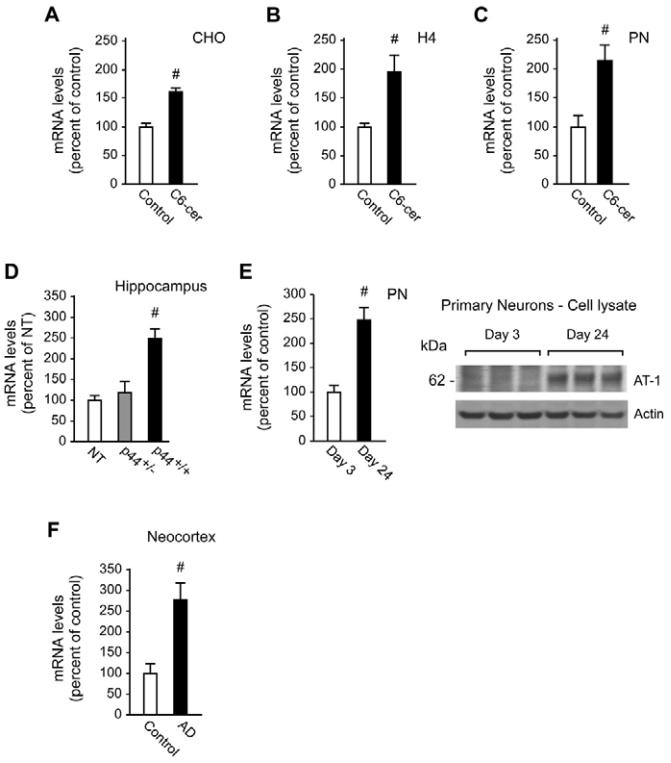

Fig. 8. AT-1 is upregulated by ceramide treatment of cultured cells and under conditions that are typically associated with high levels of endogenous ceramide. (**A**) CHO cells were treated with ceramide (C6-cer; 10 μM) prior to quantitative real-time PCR. Gene expression levels were normalized against GAPDH and results are expressed as percent of control + s.e.m. (n=5). (**B**) The experiment described in A was repeated in H4 cells. Gene expression levels were normalized against GAPDH and results are expressed as percent of control + s.e.m. (n=5). (**C**) The experiment described in A was repeated in cultured neurons (PN, primary neurons). Gene expression levels were normalized against actin and results are expressed as percent of control + s.e.m. (n=5). (**D**) Real-time determination of *AT-1* mRNA in the hippocampus of non-transgenic (NT), $p44^{+/-}$ and $p44^{+/+}$ transgenic mice. Gene expression levels were normalized against actin and results are expressed as percent of control + s.e.m. (n=4). (**E**) Hippocampal neurons were cultured in vitro for 3 and 24 days prior to real-time mRNA (left panel) and western blot (right panel) analysis of endogenous AT-1 levels. Gene expression levels were normalized against actin and results are expressed as percent of day 3 (n=10) + s.e.m. (**F**) cDNA produced from brain tissue (frontal cortex) of late-onset AD patients (n=5) and age-matched controls (n=5) was analyzed by quantitative real-time PCR. Results were normalized against GAPDH and are expressed as percent of age-matched controls + s.e.m. $^{\#}P<0.005$.

threefold) in those brain areas that are affected by AD neuropathology (Cutler et al., 2004; Han et al., 2002) (reviewed in Puglielli, 2008). Therefore, we decided to compare the mRNA levels detected in the frontal lobe of five AD patients (average age: 87; age range: 85–93) and five age-matched controls (average age: 88; age range: 86–91). There was a marked difference, with AD patients displaying an approximately threefold increase in the mRNA levels of *AT-1* (Fig. 8F). Although these results might indicate disease-relevant functions, they do not prove a direct cause-effect type of relationship between AT-1 levels and/or activity and AD neuropathology. In fact, any result obtained with post-mortem AD tissue is heavily influenced by the long duration of the disease, which could affect the genetic profile of the tissue. However, it is important to consider that *AT-1* was also found upregulated in the motor neurons of ALS patients (Jiang et al., 2007), suggesting a possible involvement in general mechanisms involved with neurodegeneration. In fact, AD and ALS differ at the mechanistic level but share common disease-relevant features, such as disruption of axonal transport, synaptic-cargo impairment, disposal of aberrant protein aggregates and organelle damage (reviewed in De Vos et al., 2008; Wong et al., 2002). Additionally, *AT-1* can be upregulated as part of the ER stress response (Shaffer et al., 2004), which appears dysfunctional in both AD and ALS neuropathology (Lindholm et al., 2006).

Discussion

The results described here support the conclusion that AT-1 is the ER membrane acetyl-CoA transporter and that its function is essential for the normal physiology of the cell. The recent identification of a missense mutation in *AT-1* associated with SPG42 and the fact that *AT-1* is upregulated in chronic neurodegenerative diseases such as sporadic ALS and late-onset (sporadic) AD point to a crucial role in disorders that are characterized by neuronal dysfunction and/or loss.

Although initially associated with nuclear and cytosolic proteins, covalent acetylation of the ε-amino group of lysine residues also occurs in the mitochondria (Schwer et al., 2006) and in the early secretory pathway (Costantini et al., 2007). In the secretory pathway, it appears to function as a new form of post-translational regulation of membrane proteins. We initially identified the acetylation machinery while analyzing the metabolism of BACE1 (Costantini et al., 2007). Following that initial finding, we have also shown that two additional membrane proteins, LDLR (Jonas et al., 2008) and APP (present study), undergo the same process.

The folding efficiency of a nascent membrane or secreted protein is enhanced by transient or permanent post-translational modifications that occur in the early secretory pathway. These modifications work in association with chaperones and proteolytic enzymes. The former protect or sequester the nascent protein, whereas the latter dispose of misfolded protein intermediates (Meusser et al., 2005; Trombetta and Parodi, 2003). In the case of BACE1, the nascent protein needs to be acetylated in the ER by two acetyltransferases, ATase1 and ATase2, which appear to act both as modifying enzymes and chaperones that protect BACE1 acetylated intermediates from PCSK9-dependent degradation (Jonas et al., 2008; Ko and Puglielli, 2009). Only the acetylated intermediates of nascent BACE1 are able to reach the Golgi complex, where they are deacetylated by a Golgi-resident deacetylase (Costantini et al., 2007). By contrast, non-acetylated intermediates are retained and degraded in a post-ER compartment, most probably the ERGIC (Jonas et al., 2008).

The post-translational events that occur in the early secretory pathway are crucial for the correct assembly of membrane and secreted proteins. As such, the widespread cell death associated with the downregulation of *AT-1* in cultured cells as well as the neuronal degeneration caused by apparent haploinsufficiency of *AT-1* in autosomal SPG42 is easily conceivable. The preferential association between changes in AT-1 levels and/or activity and neurological disorders might be due to the constant need of neuronal cells to synthesize and transport membrane and/or secreted proteins, making them more susceptible to disruption of the secretory pathway. However, AT-1 is also upregulated during the differentiation of B-cells into immunoglobulin-secreting plasma

cells, a process that involves dramatic reorganization and expansion of the ER and activation of ER stress, with the sole purpose of synthesizing and secreting a large quantity of correctly folded immunoglobulin (Shaffer et al., 2004).

ER stress, which can be initiated by overloading the secretory machinery and/or accumulating unfolded or misfolded proteins, typically activates the UPR to remove toxic aggregates. However, when insufficient, the UPR can also lead to cell death. As such, a defect in acetyl-CoA transport into the ER lumen would impede acetylation of nascent proteins that require this form of modification and result in their abnormal accumulation in the secretory pathway with consequent cellular toxicity. In this regard, it is important to point out that we are currently dissecting the ER stress signaling machinery responsible for the functional regulation of AT-1. Future work in this area might help understand the precise role of lysine acetylation of nascent membrane and/or secreted proteins as part of the UPR.

Autophagy is a general process that allows degradation and/or turnover of subcellular components (He and Klionsky, 2009). In addition to starvation and growth-factor deprivation, autophagy is activated during ER stress to dispose of large quantities of expanded ER that result from the abnormal accumulation of unfolded proteins (He and Klionsky, 2009). Evidence in yeast and mammalian cells indicates that autophagy is essential in maintaining ER homeostasis under the above conditions (Bernales et al., 2006; Ding et al., 2007; Ogata et al., 2006). Emerging data indicate that the ER membrane itself is involved in the generation of the autophagic membrane (Axe et al., 2008), thus explaining the close proximity of emerging autophagosomes to the expanded and enlarged ER structures. The dramatic activation of autophagy upon downregulation of AT-1 points to a crucial role of the ER-based acetylation machinery in maintaining ER homeostasis. Our previous work with BACE1 loss-of-acetylation and gain-of-acetylation mutants indicates that the transient acetylation of nascent BACE1 is essential for correct maturation of the nascent protein (Costantini et al., 2007). The fact that many proteins are acetylated in the ER (Fig. 6) indicates that the above events are not limited to BACE1. As such, global failure of the machinery could impede the maturation of nascent membrane and/or secreted proteins that undergo transient acetylation of the ε-amino group of lysine residues, with consequent activation of the UPR, expansion of the ER and activation of autophagy.

Materials and Methods

Plasmid constructs

Human AT-1 (NM_004733) cDNA was obtained from Origene (SC117182) and cloned into pcDNA3.1AMyc/His (Invitrogen) and pcDNA3.1V5/His/TOPO (Invitrogen).

Animals

Non-transgenic and homozygous *Pcsk9*$^{-/-}$ mice (B6;129S6-*Pcsk9tm1Jdh*/J; stock no. 005993) were from The Jackson Laboratory. *p44*$^{+/+}$ and *p44*$^{+/-}$ mice have been described previously (Costantini et al., 2006; Maier et al., 2004; Pehar et al., 2010). Animals (males) were 2.5 months old when sacrificed. Brains were collected and processed as previously described (Jonas et al., 2008). Animal experiments were carried out in accordance with the National Institutes of Health Guide for the Care and Use of Laboratory Animals and were approved by the Institutional Animal Care and Use Committee of the University of Wisconsin-Madison.

Cell cultures

Human neuroglioma (H4) and Chinese hamster ovary (CHO) cell lines were grown in Dulbecco's modified Eagle's medium (DMEM) supplemented with 10% Fetal Bovine Serum and 1% penicillin/streptomycin (Mediatech). Stably transfected cells were supplemented with 0.8% G418 sulfate. For siRNA treatment, cells were plated at a density of 6×10^4–10^6 per well and incubated from 2 to 6 days with 25 nM siRNA against *AT-1* (SI00723289; SI03186631; Hs_SLC33A1_5, Qiagen) in HiPerfect reagent (Qiagen). Non-silencing siRNA (AllStars Negative Control, Qiagen) was used as control. siRNA was applied every 2 days during the 6-day experiments. Hippocampal neurons were isolated from embryonic day 15 (E15) mice and cultured in vitro for 3 or 24 days as previously described (Costantini et al., 2005; Costantini et al., 2006). Cells were harvested and analyzed by western blot or real time-PCR, as described below. For ceramide treatment, primary neurons were cultured at a density of 32,000 cells/cm^2; after 3 days, cultures were treated with 10 μM C6 ceramide (Matreya) for 16 hours. An identical treatment was used for CHO and H4 cells. Total RNA was isolated using the RNAqueous-4PCR kit (Ambion-Invitrogen). Cell death was assessed with the Live/Dead Cell Viability/Cytotoxicity Kit (Invitrogen) and by direct cell counting.

Antibodies and western blotting

Protein electrophoresis was performed as described before (Costantini et al., 2005; Costantini et al., 2006; Jonas et al., 2008; Ko and Puglielli, 2009) on a NuPAGE system using 4–12% Bis-Tris gels (Invitrogen). The following primary antibodies were used at 1:1000 dilution in 3% bovine serum albinum (BSA) in TBST (10 mM Tris, pH 8, 150 mM NaCl, 0.1% Tween-20): antibody against acetylated lysine (Cell Signaling 9441, polyclonal), anti-APP C-terminal Fragment (C99) (Chemicon ab5352, polyclonal), anti-APP clone 4E12 (MBL M066-3, monoclonal), anti-AT1/SLC33A1 (M07) clone 3A4 (AbNova, H00009197-M07, monoclonal), anti-AT1/SLC33A1 (B01P) (AbNova, H00009197-B01P, polyclonal), anti-BACE1 (Abcam ab2077, polyclonal), anti-LDLR (polyclonal; generous gift from Alan Attie, University of Wisconsin-Madison, Madison, WI, USA) (Jonas et al., 2008), anti-beta actin (Cell Signaling 4967, polyclonal), anti-calreticulin (Abcam ab12227, polyclonal), anti-c-Myc (Sigma C3956, polyclonal), anti-Early Endosomal Antigen 1 (EEA1) (BD Transduction 610456, monoclonal), anti-ERGIC 53 (Sigma E1031, polyclonal) and anti-Syntaxin6 3D10 (Abcam ab12370, monoclonal). HRP-conjugated anti-mouse or anti-rabbit secondary antibodies were used at 1:6000 dilution in 3% BSA/TBST (GE Healthcare). Chemiluminescent detection was performed with Lumiglo (KPL) or ECL Plus (GE Healthcare). In the experiments involving *Pcsk9*$^{-/-}$ mice, samples were imaged and quantified with the LiCor Odyssey Infrared Imaging System (LI-COR Biosciences) as described before (Jonas et al., 2008).

Real-time PCR

Total RNA was isolated using RNeasy Plus Mini Kit (Qiagen), unless otherwise specified. One μg of total RNA was randomly reverse transcribed using SuperScript III reverse transcriptase (Invitrogen) according to the manufacturer's instructions. Quantitative PCRs were carried out in a LightCycler480 Real-time PCR System (Roche) using LightCycler480 SYBR Green I Master Mix (Roche). The cycling parameters were as follows: 95°C, 10 seconds; 55°C, 10 seconds; 72°C, 15 seconds, for a maximum of 40 cycles. Controls without reverse transcription were included in each assay. PCR primers specific to each gene were as follows: AT1-mouse, 59-TACGTGCTTCAGGGCATTCC-39 and 59-CTGAAGAAAGCCTGGTCTGT-ATAGC-39 (95 bp); actin-mouse, 59-CATGAAGATCCTGACCGAGCGTG-39 and 59-TCTGCTGGAAGGTGGACAGTGAGG-39 (497 bp); AT1-human, 59-CAGGCGGTTGGGATGACAGT-39 and 59-AAGATTTGCGACGACCGAAGTT-39 (333 bp); glyceraldehyde-3-phosphate dehydrogenase (GAPDH)-human, 59-TTTGTCAAGCTCATTTCCTGGTA-39 and 59-TTCAAGGGGTCTACATG-GCAACTG-39 (225 bp). AT-1 expression levels were normalized against actin or GAPDH levels and are expressed as percent of control.

The mRNA of AD patients and age-matched controls was a generous gift of Craig Atwood (University of Wisconsin-Madison, Madison, WI, USA).

Acetyl-CoA membrane transport

Subcellular fractionation was performed as described (Costantini et al., 2007; Jonas et al., 2008; Ko and Puglielli, 2009). Individual fractions were immediately centrifuged at 100,000 ***g*** (25 psi) for 15 minutes in an air-driven ultracentrifuge (Airfuge; Beckman), and pellets were resuspended in isotonic/cryogenic buffer (0.25 M sucrose and 10 mM Tris/HCl pH 7.4). Acetyl-CoA transport into intact native vesicles was performed as already described in detail (Costantini et al., 2007). In the case of competition assays, purified native ER fractions were incubated in the presence of 10 μm [^{3}H] acetyl-CoA and increasing concentrations of CoA (Sigma), ATP (Sigma), UDP-galactose (MP Biomedicals) and sodium acetate (Sigma) in isotonic/cryogenic buffer. Reactions were run as in a typical membrane transport assay (Costantini et al., 2007).

In vitro reconstitution

For the reconstitution of AT-1 activity into artificial liposomes, transgenic AT-1 was purified from stably transfected cells with the Myc-Tag IP/Co-IP Kit (Pierce) as suggested by the manufacturer and already described in our previous work (Costantini et al., 2007). Briefly, cell lysates from CHO cells stably transfected with AT-1 were loaded onto the above anti-Myc immobilized column, washed and eluted by lowering the pH to 2.0. The pH was immediately neutralized by adding 10 μl of neutralizing buffer (1 M Tris pH 9.5) per 200 μl of elution buffer. 18 μl of the elution was gently mixed with 50 μl of artificial liposomes and reconstituted with five cycles of freeze-thaw in an acetone-dry ice bath, as described before (Mandon et al., 1994; Puglielli and Hirschberg, 1999; Puglielli et al., 1999a; Puglielli et al., 1999b). Liposomes were made of a mixture of phosphatidylcholine:phosphatidylethanolamine:

phosphatidylserine (55:30:15). Phosphatidylethanolamine and phosphatidylserine were added to mimic more closely the natural lipid environment of the ER membrane (Yunghans et al., 1970). In fact, previous work with the ER membrane ATP transporter suggests that, in contrast to Golgi membrane transporters (Mandon et al., 1994; Puglielli and Hirschberg, 1999; Puglielli et al., 1999a), ER membrane transporters are not efficiently reconstituted into simple phosphatidylcholine artificial liposomes (Guillen and Hirschberg, 1995). Reconstituted proteoliposomes were assayed for acetyl-CoA transport immediately after the last freeze-thaw cycle. As control, transport was also assayed in liposomes alone (in the absence of AT-1) and in mixtures of liposomes plus AT-1 without freeze-thaw-mediated reconstitution. Finally, as additional control, a cell extract from control (non-transfected) cells was also loaded onto the above anti-Myc column and the elution volume was reconstituted into artificial liposomes.

Trypsin digestion

Purified ER vesicles were incubated for 60 minutes at 25°C with trypsin (Sigma) at a final concentration of 1 μg of protease per μg of ER or Golgi proteins. Digestion was halted by the addition of anti-trypsin specific inhibitor (Sigma) and by lowering the temperature to 0–4°C. The anti-trypsin inhibitor was used at the final concentration of 1 μg of inhibitor per μg of protease. Trypsin digestion was performed in the presence or absence of 0.05% Triton X-100.

Electron microscopy

Transmission electron microscopy was performed at the Electron Microscopy Facility of the William S. Middleton Memorial Veterans Hospital (Madison, WI) and University of Wisconsin-Madison, as described before (Oberley et al., 2008). All supplies and reagents were from Electron Microscopy Sciences (Hatfield, PA). Sections were observed using a transmission electron microscope (Hitachi H-600) operated at 75 kV.

Aβ determination

For Aβ determination in the conditioned medium, CHO cells were plated in six-well Petri dishes. When 80–90% confluent, cells were washed in PBS and incubated in 1 ml of fresh medium for 48 hours. Secreted Aβ was determined as described before by using a standard sandwich enzyme-linked immunosorbent assay (ELISA) system designed for the detection of rodent Aβ (Costantini et al., 2006; Costantini et al., 2005; Jonas et al., 2008; Ko and Puglielli, 2009; Puglielli et al., 2003).

Statistical analysis

Results are always expressed as mean of the indicated number of determinations. Unless specified, the data were analyzed by ANOVA and Student's *t*-test comparison, using GraphPad InStat3 software. Statistical significance was reached at $P<0.05$.

We thank Carlos B. Hirschberg and Nansi Jo Colley for the critical reading of an early version of this manuscript. We are grateful to Jamie Swanlund for help with electron microscopy, and to Kate Shields and Sinziana Cornea for laboratory support. We are also grateful to Ed Chapman's laboratory for the generation of artificial liposomes. This research was supported by the NIH/NIA (AG028569 and AG033514) to L.P. and by resources and facilities of the William S. Middleton Memorial Veterans Hospital, Madison, WI. Deposited in PMC for release after 12 months.

References

Abisambra, J. F., Fiorelli, T., Padmanabhan, J., Wefes, I., Neame, P., Goodwin, B., Norden, M. and Potter, H. (2009). APP over-expression affects the localization of PCSK9 and LDLR. Program no. 43.5/D26, Society for Neuroscience 2009 Annual Meeting, Chicago, IL

Axe, E. L., Walker, S. A., Manifava, M., Chandra, P., Roderick, H. L., Habermann, A., Griffiths, G. and Ktistakis, N. T. (2008). Autophagosome formation from membrane compartments enriched in phosphatidylinositol 3-phosphate and dynamically connected to the endoplasmic reticulum. *J. Cell Biol.* **182**, 685-701.

Bernales, S., McDonald, K. L. and Walter, P. (2006). Autophagy counterbalances endoplasmic reticulum expansion during the unfolded protein response. *PLoS Biol.* **4**, e423.

Berninsone, P. M. and Hirschberg, C. B. (2000). Nucleotide sugar transporters of the Golgi apparatus. *Curr. Opin. Struct. Biol.* **10**, 542-547.

Carey, D. J. and Hirschberg, C. B. (1981). Topography of sialoglycoproteins and sialyltransferases in mouse and rat liver Golgi. *J. Biol. Chem.* **256**, 989-993.

Costantini, C., Weindruch, R., Della Valle, G. and Puglielli, L. (2005). A TrkA-to-p75NTR molecular switch activates amyloid beta-peptide generation during aging. *Biochem. J.* **391**, 59-67.

Costantini, C., Scrable, H. and Puglielli, L. (2006). An aging pathway controls the TrkA to p75(NTR) receptor switch and amyloid beta-peptide generation. *EMBO J.* **25**, 1997-2006.

Costantini, C., Ko, M. H., Jonas, M. C. and Puglielli, L. (2007). A reversible form of lysine acetylation in the ER and Golgi lumen controls the molecular stabilization of BACE1. *Biochem. J.* **407**, 383-395.

Cutler, R. G., Kelly, J., Storie, K., Pedersen, W. A., Tammara, A., Hatanpaa, K., Troncoso, J. C. and Mattson, M. P. (2004). Involvement of oxidative stress-induced abnormalities in ceramide and cholesterol metabolism in brain aging and Alzheimer's disease. *Proc. Natl. Acad. Sci. USA* **101**, 2070-2075.

De Vos, K. J., Grierson, A. J., Ackerley, S. and Miller, C. C. (2008). Role of axonal transport in neurodegenerative diseases. *Annu. Rev. Neurosci.* **31**, 151-173.

Ding, W. X., Ni, H. M., Gao, W., Hou, Y. F., Melan, M. A., Chen, X., Stolz, D. B., Shao, Z. M. and Yin, X. M. (2007). Differential effects of endoplasmic reticulum stress-induced autophagy on cell survival. *J. Biol. Chem.* **282**, 4702-4710.

Farquhar, M. G. and Hauri, H.-P. (1997). Protein sorting and vesicular traffic in the Golgi apparatus. In *The Golgi Apparatus* (ed. E. G. Berger and J. Roth), pp. 63-129. Basel: Birkhäuser Verlag.

Guillen, E. and Hirschberg, C. B. (1995). Transport of adenosine triphosphate into endoplasmic reticulum proteoliposomes. *Biochemistry* **34**, 5472-5476.

Han, X. M., Holtzman, D., McKeel, D. W., Jr, Kelley, J. and Morris, J. C. (2002). Substantial sulfatide deficiency and ceramide elevation in very early Alzheimer's disease: potential role in disease pathogenesis. *J. Neurochem.* **82**, 809-818.

He, C. and Klionsky, D. J. (2009). Regulation mechanisms and signaling pathways of autophagy. *Annu. Rev. Genet.* **43**, 67-93.

Hirabayashi, Y., Kanamori, A., Nomura, K. H. and Nomura, K. (2004). The acetyl-CoA transporter family SLC33. *Pflugers Arch.* **447**, 760-762.

Hirschberg, C. B., Robbins, P. W. and Abeijon, C. (1998). Transporters of nucleotide sugars, ATP, and nucleotide sulfate in the endoplasmic reticulum and Golgi apparatus. *Annu. Rev. Biochem.* **67**, 49-69.

Jiang, Y. M., Yamamoto, M., Tanaka, F., Ishigaki, S., Katsuno, M., Adachi, H., Niwa, J., Doyu, M., Yoshida, M., Hashizume, Y. et al. (2007). Gene expressions specifically detected in motor neurons (dynactin 1, early growth response 3, acetyl-CoA transporter, death receptor 5, and cyclin C) differentially correlate to pathologic markers in sporadic amyotrophic lateral sclerosis. *J. Neuropathol. Exp. Neurol.* **66**, 617-627.

Jonas, M. C., Costantini, C. and Puglielli, L. (2008). PCSK9 is required for the disposal of non-acetylated intermediates of the nascent membrane protein BACE1. *EMBO Rep.* **9**, 916-922.

Kanamori, A., Nakayama, J., Fukuda, M. N., Stallcup, W. B., Sasaki, K., Fukuda, M. and Hirabayashi, Y. (1997). Expression cloning and characterization of a cDNA encoding a novel membrane protein required for the formation of O-acetylated ganglioside: a putative acetyl-CoA transporter. *Proc. Natl. Acad. Sci. USA* **94**, 2897-2902.

Ko, M. H. and Puglielli, L. (2007). The sterol carrier protein SCP-x/pro-SCP-2 gene has transcriptional activity and regulates the Alzheimer disease gamma-secretase. *J. Biol. Chem.* **282**, 19742-19752.

Ko, M. H. and Puglielli, L. (2009). Two endoplasmic reticulum (ER)/ER golgi intermediate compartment-based lysine acetyltransferases post-translationally regulate BACE1 Levels. *J. Biol. Chem.* **284**, 2482-2492.

Lin, P., Li, J., Liu, Q., Mao, F., Qiu, R., Hu, H., Song, Y., Yang, Y., Gao, G., Yan, C. et al. (2008). A missense mutation in SLC33A1, which encodes the acetyl-CoA transporter, causes autosomal-dominant spastic paraplegia (SPG42). *Am. J. Hum. Genet.* **83**, 752-759.

Lindholm, D., Wootz, H. and Korhonen, L. (2006). ER stress and neurodegenerative diseases. *Cell Death Differ.* **13**, 385-392.

Maier, B., Gluba, W., Bernier, B., Turner, T., Mohammad, K., Guise, T., Sutherland, A., Thorner, M. and Scrable, H. (2004). Modulation of mammalian life span by the short isoform of p53. *Genes Dev.* **18**, 306-319.

Mandon, E. C., Milla, M. E., Kempner, E. and Hirschberg, C. B. (1994). Purification of the Golgi adenosine 39-phosphate 59-phosphosulfate transporter, a homodimer within the membrane. *Proc. Natl. Acad. Sci. USA* **91**, 10707-10711.

Masumoto, H., Hawke, D., Kobayashi, R. and Verreault, A. (2005). A role for cell-cycle-regulated histone H3 lysine 56 acetylation in the DNA damage response. *Nature* **436**, 294-298.

Meusser, B., Hirsch, C., Jarosch, E. and Sommer, T. (2005). ERAD: the long road to destruction. *Nat. Cell Biol.* **7**, 766-772.

Oberley, T. D., Swanlund, J. M., Zhang, H. J. and Kregel, K. C. (2008). Aging results in increased autophagy of mitochondria and protein nitration in rat hepatocytes following heat stress. *J. Histochem. Cytochem.* **56**, 615-627.

Ogata, M., Hino, S., Saito, A., Morikawa, K., Kondo, S., Kanemoto, S., Murakami, T., Taniguchi, M., Tanii, I., Yoshinaga, K. et al. (2006). Autophagy is activated for cell survival after endoplasmic reticulum stress. *Mol. Cell. Biol.* **26**, 9220-9231.

Pehar, M., O'Riordan, K. J., Burns-Cusato, M., Andrzejewski, M. E., del Alcazar, C. G., Burger, C., Scrable, H. and Puglielli, L. (2010). Altered longevity-assurance activity of p53:p44 in the mouse causes memory loss, neurodegeneration and premature death. *Aging Cell* **9**, 174-190.

Puglielli, L. (2008). Aging of the brain, neurotrophin signaling, and Alzheimer's disease: is IGF1-R the common culprit? *Neurobiol. Aging* **29**, 795-811.

Puglielli, L. and Hirschberg, C. B. (1999). Reconstitution, identification, and purification of the rat liver golgi membrane GDP-fucose transporter. *J. Biol. Chem.* **274**, 35596-35600.

Puglielli, L., Mandon, E. C. and Hirschberg, C. B. (1999a). Identification, purification, and characterization of the rat liver golgi membrane ATP transporter. *J. Biol. Chem.* **274**, 12665-12669.

Puglielli, L., Mandon, E. C., Rancour, D. M., Menon, A. K. and Hirschberg, C. B. (1999b). Identification and purification of the rat liver Golgi membrane UDP-N-acetylgalactosamine transporter. *J. Biol. Chem.* **274**, 4474-4479.

Puglielli, L., Ellis, B. C., Saunders, A. J. and Kovacs, D. M. (2003). Ceramide stabilizes beta-site amyloid precursor protein-cleaving enzyme 1 and promotes amyloid beta-peptide biogenesis. *J. Biol. Chem.* **278**, 19777-19783.

Rashid, S., Curtis, D. E., Garuti, R., Anderson, N. N., Bashmakov, Y., Ho, Y. K., Hammer, R. E., Moon, Y. A. and Horton, J. D. (2005). Decreased plasma cholesterol and hypersensitivity to statins in mice lacking Pcsk9. *Proc. Natl. Acad. Sci. USA* **102**, 5374-5379.

Schwer, B., Bunkenborg, J., Verdin, R. O., Andersen, J. S. and Verdin, E. (2006). Reversible lysine acetylation controls the activity of the mitochondrial enzyme acetyl-CoA synthetase 2. *Proc. Natl. Acad. Sci. USA* **103**, 10224-10229.

Shaffer, A. L., Shapiro-Shelef, M., Iwakoshi, N. N., Lee, A. H., Qian, S. B., Zhao, H., Yu, X., Yang, L., Tan, B. K., Rosenwald, A. et al. (2004). XBP1, downstream of Blimp-1, expands the secretory apparatus and other organelles, and increases protein synthesis in plasma cell differentiation. *Immunity* **21**, 81-93.

Trombetta, E. S. and Parodi, A. J. (2003). Quality control and protein folding in the secretory pathway. *Annu. Rev. Cell Dev. Biol.* **19**, 649-676.

Wong, P. C., Cai, H., Borchelt, D. R. and Price, D. L. (2002). Genetically engineered mouse models of neurodegenerative diseases. *Nat. Neurosci.* **5**, 633-639.

Yunghans, W. N., Keenan, T. W. and Morré, D. J. (1970). Isolation of Golgi apparatus from rat liver. III. Lipid and protein composition. *Exp. Mol. Pathol.* **12**, 36-45.